CARBON 59 (2013) 439–447

Available at www.sciencedirect.com

SciVerse ScienceDirect

journal homepage: www.elsevier.com/locate/carbon

Hydrogen-excluded graphene synthesis *via* atmospheric pressure chemical vapor deposition

Yong Cheol Shin [a], *Jing Kong* [b,*]

[a] *Department of Materials Science and Engineering, Massachusetts Institute of Technology, Cambridge, MA 02139, USA*
[b] *Department of Electrical Engineering and Computer Science, Massachusetts Institute of Technology, Cambridge, MA 02139, USA*

ARTICLE INFO

Article history:
Received 12 February 2013
Accepted 18 March 2013
Available online 26 March 2013

ABSTRACT

The morphology of graphene synthesized *via* atmospheric pressure chemical vapor deposition (APCVD) process was investigated with respect to the hydrogen introduction in each process step. A pristine monolayer graphene was obtained in the condition where hydrogen was excluded in all the steps. The study of growth mechanism of this hydrogen-excluded APCVD process suggests that hydrogen plays a critical role in determining the rate-limiting step, which further determines whether or not a monolayer graphene can be achieved, irrespective to the roughness of the surface. Particularly, the dominant kinetic regime changed, depending on the introduction of hydrogen in the growth step. Finally, electric properties of the graphene *via* the hydrogen-excluded APCVD process were characterized and compared with the one *via* the low pressure CVD process, along with the characterization of etch pits in a graphene-passivated etch test. The resulted better performance of the former graphene in both cases suggests that this method can be considered as an alternative but easier route for the synthesis of monolayer graphene.

1. Introduction

Graphene, a monatomic plane composed of sp^2-hybridized carbon atoms in a hexagonal arrangement, have been a material of intense interest for its remarkable electrical [1,2], chemical [3], mechanical [4], and thermal properties [5]. Various efforts to utilize it for promising applications such as photovoltaic devices [6], transistors [7,8], flat panel display [9] or electrochemical energy storage[10], have been devoted. Among the methods to synthesize graphene, metal catalyst-mediated chemical vapor deposition (CVD) process based on pyrolysis of hydrocarbon [9,11–13] suggests a feasible process to industrialize due to its high compatibility to conventional industries and suitability for large-area fabrication, while maintaining the excellent material properties [1]. Particularly, the discovery of copper as the most optimal catalyst that can lead to form a pristine monolayer graphene [12] was revolutionary in the respect that opened up the applicability of the monolayer graphene to practical devices in large area [9]. Under a low pressure CVD (LPCVD) process, the growth mechanism is known as a self-limiting process based on a copper-mediated surface reaction of pyrolysed carbon atoms [12]. There have also been various attempts to synthesize graphene under atmospheric (AP) conditions as in general APCVD is easier and cheaper to implement than LPCVD. Monolayer graphene was only obtained when highly diluted methane (~ppm) gas was used for the growth [14,15]. In this work, by investigating the graphene growth mechanism and the role of hydrogen in the APCVD process, it was found that when hydrogen is excluded in the growth process, surface reaction becomes the rate-limiting step of the APCVD process thereby leading to the preferred formation of monolayer graphene. Further investigations were carried out to elucidate this understanding and the quality of these monolayer

* *Corresponding author:* Fax: +1 617 324 5293.
E-mail address: jingkong@mit.edu (J. Kong).
0008-6223/$ - see front matter
http://dx.doi.org/10.1016/j.carbon.2013.03.037

graphene films were found to be better than the typical LPCVD grown monolayer graphene through electrical and etch pit density characterizations.

2. Results and discussion

The general process of the graphene synthesis by the APCVD process conducted in this article is described in the following [14]: Synthesis steps consisted of purging, heating, annealing, growth, and cooling. For the heating step, the furnace temperature ramped up from room temperature to 1000 °C under inert gas. The annealing step was used to remove the native oxide on the copper surface as well as to increase the grain size of the copper substrate. The growth step was held at the same temperature as the annealing step, and subsequently, graphene formed in this step with methane gas as a carbonaceous source. Finally, by terminating the methane feedstock and isolating the reactor chamber (a fused quartz tube) from the furnace promptly, the copper foil and the chamber were cooled down to room temperature under inert gas atmosphere. To investigate the effect of hydrogen, four types of graphene samples were prepared depending on whether there was exposure to hydrogen in each of the four steps, while the flow rate of argon as an inert carrier gas was fixed during all the steps. The detailed composition of gases for sample preparation is given in Table 1. The four conditions are labeled as A1–A4, A1 corresponds to having hydrogen in all steps ("H_2_In_All"), A2 corresponds to not having hydrogen in the growth step but the other three steps ("H_2_NOTIn_Growth"), A3 corresponds to excluding H_2 in all the four steps ("H_2_Excluded"), whereas A4 corresponds to having H_2 only in the growth step but not the other steps ("H_2_ONLYIn_Growth"). After the synthesis finished, the samples were transferred onto either thermally oxidized silicon or transparent boron silicate substrates for analysis.

2.1. The morphology of graphene samples transferred on SiO_2/Si

Fig. 1 shows the optical microscope (OM) images of four graphene samples (transferred on SiO_2/Si substrate) prepared by APCVD with different hydrogen feedstock as indicated in Table 1. It is highly remarkable that a coarse multilayer graphene was obtained when hydrogen was flowed in all the synthesis steps (Fig. 1(a), A1 condition in Table 1) while a pristine monolayer graphene was observed when hydrogen was completely excluded in the process (Fig. 1(c), A3 condition in Table 1). The equivalent number of layer was calculated by measuring the transmittance of the samples transferred on a transparent boron silicate substrate. Since the specific transmittance of the sample by A3 condition was 96.5% at 550 nm of the wavelength, monolayer was estimated. Although this value is a little lower than the theoretical value for a monolayer, 97.7% [16–18], it is consistent with LPCVD grown monolayer graphene sample, and it appears to be due to wrinkles formed upon the cooling step [18] or defects on the graphene such as a polymer residue by the transfer process. On the other hand, the sample A1 has 85.9% of the transmittance at the same wavelength which corresponds to 5–6 eq. layers of graphene [18]. Both of the samples by A2 and A4 condition seemed to have less numbers of graphene layer than the sample by A1 condition; however, as depicted in Fig. 1(b) and (d), they were not monolayer graphene. The general trend could be divided into two aspects. First, in Fig. 1(a) and (b) where hydrogen was fed in the heating and annealing step, multilayer graphene aligned to the rolling line direction of copper foil formed. In contrast, in Fig. 1(c) and (d) where hydrogen was excluded in both of the steps, such a directional arrangement of multilayer graphene was not observed. The effect of hydrogen in the cooling step was also investigated by transposing the hydrogen flow in the cooling step with the condition in Table 1; very interestingly, no noticeable deviation from Fig. 1 was observed (See Table S1 and Fig. S1 in Supporting Information).

2.2. The morphology of copper foils with different annealing treatments

Since these morphologies might be associated with the surface of copper foil underneath, to confirm how hydrogen assist in the morphological changes of the copper surface, right after the annealing step samples were taken out of the reactor and were investigated (the two conditions studied here are: annealing with hydrogen and argon under AP (this is the condition used in A1, A2), and annealing with argon only under AP (this is the condition used in A3, A4)). The sample annealed under LP was also prepared. The corresponding optical and atomic force microscope (AFM) images are presented in Fig. 2(a–h), respectively. As expected, the surface of an as-received copper foil with rolling lines on the surface (Fig. 2(a) and (e)) was smoothened after annealing under LP (Fig. 2(b) and (f)), showing the RMS roughness change from 9.4 nm to 0.83 nm. The aspect of the morphology change of the copper surface after annealing under AP was more notable. While the formation of voids or hillocks aligned to the pattern was observed in the hydrogen and argon annealing under AP (Fig. 2(c) and (g)), the copper surface annealed with argon only under AP (Fig. 2(d) and (h)) showed a flat surface with the RMS roughness of 1.82 nm. (This slight higher

Table 1 – The graphene samples prepared by APCVD process with different composition of gases.

H_2:CH_4:Ar (sccm)	Heating	Annealing	Growth	Cooling
A1: H_2_In_All	50:0:500	50:0:500	50:3:500	50:0:500
A2: H_2_NOTIn_Growth	50:0:500	50:0:500	0:3:500	50:0:500
A3: H_2_Excluded	0:0:500	0:0:500	0:3:500	0:0:500
A4: H_2_ONLYIn_Growth	0:0:500	0:0:500	50:3:500	0:0:500

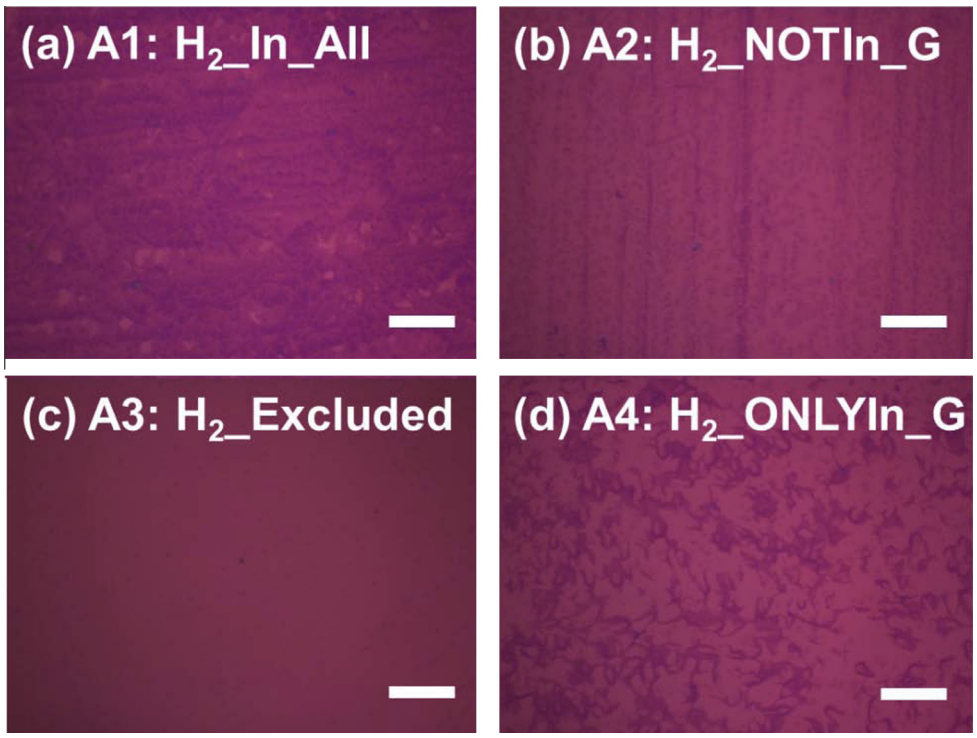

Fig. 1 – OM image of transferred graphene samples on a SiO_2/Si substrate. The composition of flow gases for (a–d) are corresponding to A1–A4 in Table 1, respectively. The scale bars are all 20 μm.

roughness than the one annealed under LP was attributed to the local faceting shown in inset of Fig. 2(h)). The same bumpy topography in Fig. 2(c) and (g) as rough as tens of nanometer indicated by the AFM analysis was also resulted in other annealing experiments carried out with a diluted hydrogen concentration (0.1% in vol.) or a forming gas (5% hydrogen in nitrogen) under AP. This suggested the roughening of the copper surface should be related to the hydrogen flowed in the heating and annealing step under AP. At this stage the mechanism of how hydrogen under AP caused the copper foil to be rougher in the annealing step is not completely clear, but there are two possible explanations, hydrogen embrittlement by degassing [19] and surface diffusion. The hydrogen embrittlement develops to copper or copper alloys during annealing with hydrogen. When the hydrogen reacts with oxygen existed as a form of copper oxide, the resulted water vapor can have high vapor pressure at the sites where this reduction reaction happens since the vapor molecules cannot diffuse through the metal. In the end, these sites are replaced by voids and cracks. Taking into account that the hydrogen embrittlement occurs between at 400 °C with 8% hydrogen and 700 °C at 1% hydrogen under AP with 1.5 h of annealing time [19], this phenomenon can be probable in the annealing condition used in A1 and A2. In addition, although the copper foil used in the experiment was 25 μm-thick, the roughening by surface diffusion should be considered because not only that the copper was poly-crystalline, but the annealing was carried out at the temperature close to the melting point of copper, 1084 °C. It should be noted that there was no change in crystallographic orientation of the copper foil preferred along [100] direction confirmed by X-ray diffraction (XRD), regardless of the annealing condition (See Fig. S2 in Supporting Information).

2.3. *Self-limiting growth characteristics of hydrogen-excluded APCVD process*

Since no noticeable change in topography was observed on the copper foil after the completion of the graphene synthesis, the graphene morphology in each growth condition could be associated with the topography of the copper foil after annealing. First, multilayer graphene aligned to the rolling direction as shown in Fig. 1(a) and (b) could be attributed to the rough surface of copper foil by hydrogen introduction in the heating and annealing step. The expectation that a rougher substrate surface will give rise to form more multilayer graphene flakes can be understood by the postulation that the general rate-limiting step of the APCVD process is not the surface reaction on the copper, but the mass transport from bulk region to surface region [14]. Furthermore, the graphene growth under APCVD is not self-limiting (in contrast to LPCVD), the roughness on the surface can cause different boundary layer thickness, and thus the growth rate is different. Therefore in this kinetic regime, the process is sensitive to the surface feature thereby leading to form multilayer graphene by the rough surface of copper foil [15] through accumulated nucleation along the rolling direction. In contrast to this, when the same type of rough surface of copper foil (i.e., annealed in hydrogen and argon under AP, Fig. 2(c) and (g)) was used in a LPCVD (1.70 Torr) graphene growth process, the resulting graphene was monolayer with the transmittance of 96.5%, in consistent with a typical

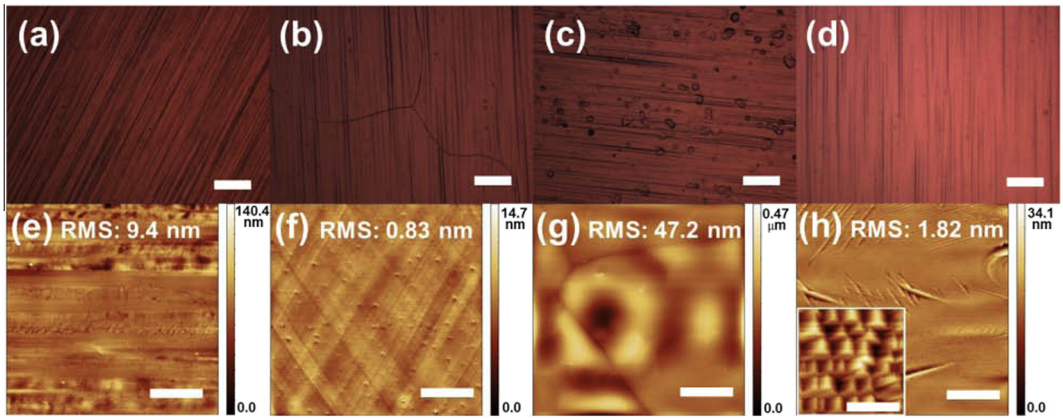

Fig. 2 – (a–d) OM image of copper foils treated with different conditions. (a) as-received, (b) after annealing under LP with hydrogen only, (c) after annealing under AP with hydrogen and argon, and (d) after annealing under AP with argon only. (e–h) are corresponding AFM images of (a–d), respectively. The scale bars of (a–d) are 100 μm and (e–h) are 5 μm while the one in the inset of (h) is 500 nm.

LPCVD growth result, which is shown in Fig. 3(a). This is because the kinetics of the LPCVD is dominated by the surface reaction on the copper surface, and the graphene growth is self-limiting [14], the effect of surface topography turned out to be not so important. With this understanding that growth kinetics needs to be considered to account for the dependence of the roughness of copper surface to the morphology of graphene, it was elucidated how a uniform monolayer graphene can be obtained in A3 condition, the hydrogen-excluded APCVD process. It was noted that when A3 condition was applied, monolayer graphene was obtained on a rougher copper surface (Fig. 2(d) and (h)) than the one annealed under LP (Fig. 2(b) and (f)) although this was much smoother than the one where A1 condition was applied (Fig. 2(c) and (e)). Even more interestingly, as can be seen in the Fig. 3(b), when the copper foil with the rough surface of Fig. 2(c) was used for A3 condition, a close-to-monolayer graphene with trace amount of multilayer flakes was also obtained. This suggested the hydrogen excluded growth likely has the similar growth kinetics to the LPCVD growth, that is, surface reaction limiting.

The graphene synthesis by a simple APCVD process is known to have a kinetically rate-liming step in the transport of gas molecules from bulk region to surface [14]. Therefore, since the growth is not self-limiting, the formation of multilayer more than a single layer is probable. This was sensitively controlled by the methane concentration, or namely, the partial pressure of methane, where monolayer graphene can be obtained with extremely low methane concentration on a highly flat surface [14,15]. However, the results we obtained here suggested that the hydrogen-excluded APCVD process had a different kinetic barrier from a usual APCVD process. In order to gain further understanding on this, first, we varied the methane concentration, fixing A3 growth condition. It was found that there was no significant difference in morphology with respect to the methane concentration, monolayer was commonly obtained. This was contrasted with the previous APCVD results [14] that the graphene morphology was highly sensitive to the methane concentration. As can be seen in Fig. 4(a–d), although the methane flow rate changed by 1, 2, 10, and 20 sccm, respectively, the resulted graphene morphologies were similar to Fig. 1(c) where 3 sccm of methane was used. This result suggested the graphene growth in the hydrogen excluded process appears to have a self-limiting nature even though it was carried out in AP. It should be also noted that within the experimented methane concentration range, it was found that a "conditioned" quartz tube where a thin copper layer was deposited on the inner wall by a LPCVD helped in obtaining a reliable uniform monolayer graphene. Together with the previous observation that a monolayer graphene was obtained in spite of the rough surface topographies of the copper foil (Fig. 3(b)), it gives further evidence that the kinetics of the hydrogen-excluded APCVD process was mainly dominated by the surface reaction on copper. This means that by excluding hydrogen in APCVD process, the dominant kinetic barrier is converted from the mass transport of gases molecules to the surface reaction such as the methane decomposition process.

2.4. *Understanding of the growth mechanism of hydrogen-excluded APCVD process*

2.4.1. *The investigation of domain shape of graphene samples at initial growth stage*

To confirm this change of the main kinetic regime by hydrogen, the domain shape of graphene was investigated by ceasing the growth within short time, before the coalescence of nuclei. Firstly, the scanning electron microscopy (SEM) images of graphene grown on a copper foil for just 3 min where A1 and A3 condition are shown in Fig. 5(a) and (b), respectively. Fig. 5(c) and (d) are the SEM images of other partially grown graphene samples on a flat 127 μm-thick Cu foil electropolished by a 75 vol.% phosphoric acid, prepared to compare with the results. The graphene shown in Fig. 5(c) was obtained after 5 min of the growth time where the similar condition to A1 was applied. Fig. 5(d) was taken after 5 min growth of LPCVD process at 1035 °C with hydrogen and methane. Detailed description of the electropolishing process and the growth conditions for Fig. 5(c) and (d) are provided in the Supporting Information. As can be seen in Fig. 5(a), in

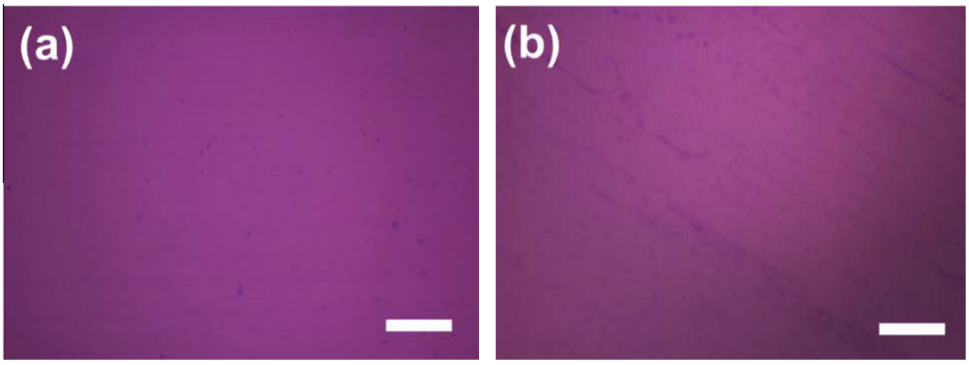

Fig. 3 – OM image of transferred graphene samples on a SiO_2/Si substrate. The graphene was synthesized by using a copper foil with rough surface shown in Fig. 2(c) where (a) LPCVD process condition was applied and (b) A3 condition (hydrogen-excluded APCVD) was applied. The scale bars are 20 μm.

the partially grown graphene where A1 condition was applied, the domain shape was not distinguishable, but instead flakes aligned to the rolling direction were observed. This directional growth continues across the grain boundaries of copper foil (See Fig. S3(a) in Supporting Information). The observation here that nucleation was prevailed on rough sites along the rolling line is consistent with the understanding that the dominant rate-limiting step for this condition (A1) was the mass transport of gas. In this sample, because the nucleation density was too high, the shape of the graphene flakes could not be recognized. Thus a flat Cu foil prepared by an electrochemical polishing process with the surface roughness of 1.5 nm was used for similar growth condition to the A1 (In order to minimize the roughening effect by hydrogen during annealing, the annealing step was skipped) to investigate the shape of the flakes. The result shown in Fig. 5(c) revealed mostly hexagon-shaped graphene nuclei. On the other hand, the partially grown graphene in the hydrogen excluded process showed lobe-shapes with six folds, illustrated in Fig. 5(b). In other attempts, fourfold morphology was also observed (See Fig. S3(c) in Supporting Information). Furthermore, as compared to Fig. 5(c) grown for 5 min, the size of each nucleus was much larger in spite of the shorter growth time of 3 min; besides, the less density of nucleus was also observed. These characteristics were consistent with the partially grown graphene in Fig. 5(d) prepared by LPCVD process. In the meantime, there have been reports on the domain shape of graphene grown by Cu-mediated CVD [20–26].

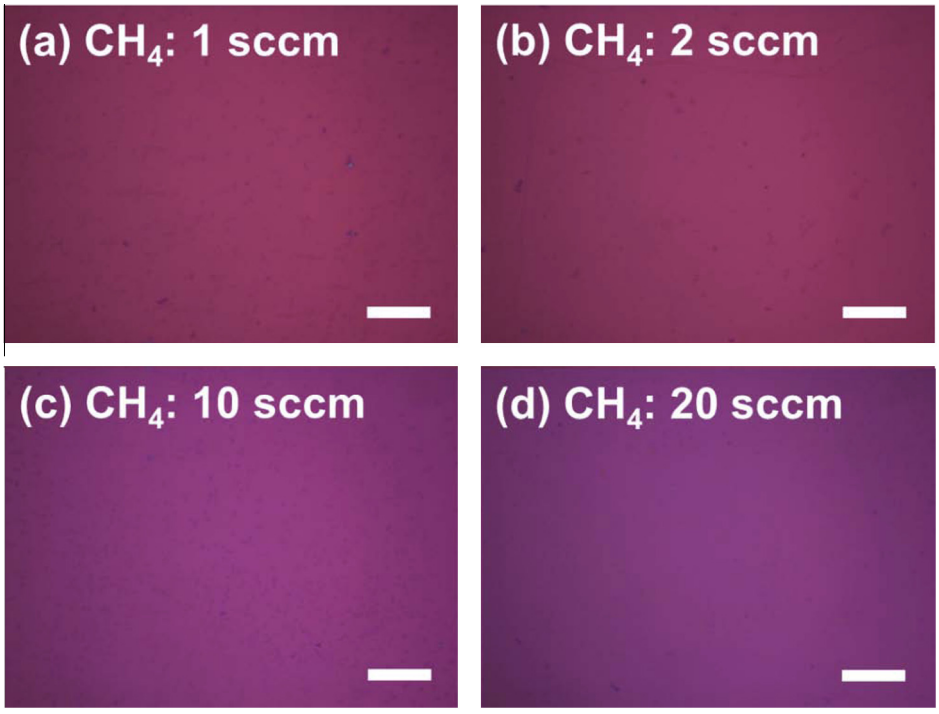

Fig. 4 – OM image of transferred graphene samples on a SiO_2/Si substrate. The samples were prepared by applying the A3 condition where hydrogen was excluded in all the steps, varying the methane flow rate. The flow rate of methane feedstock of (a–d) is, 1, 2, 10, 20 sccm, respectively. The scale bars are 20 μm.

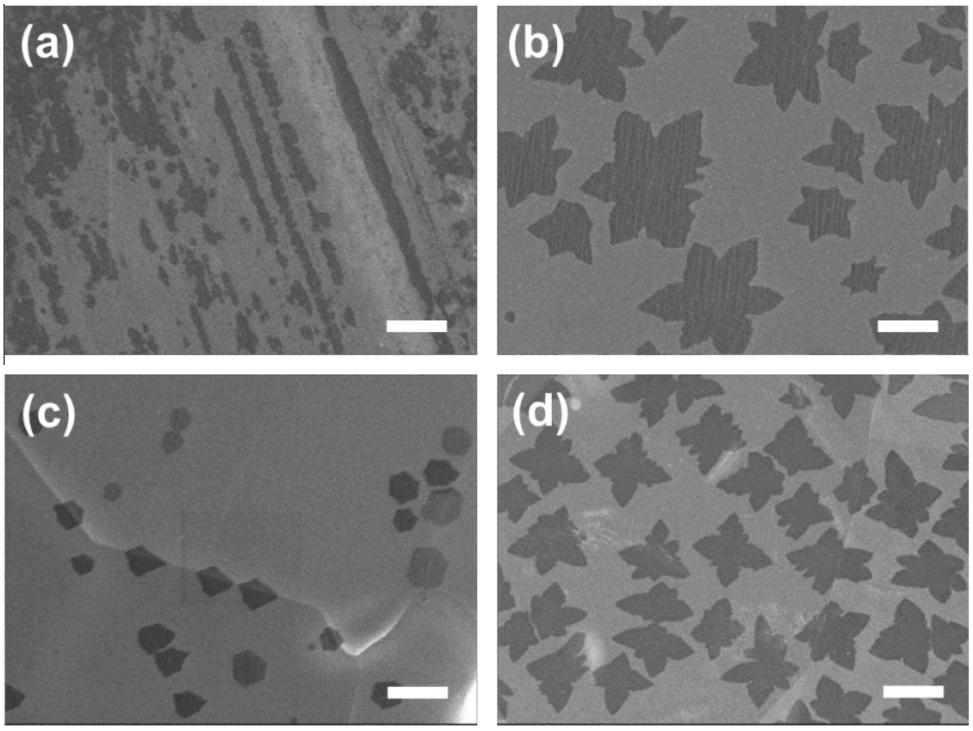

Fig. 5 – The SEM image of partially grown graphene on a copper foil. (a) and (b) are graphene grown for 3 min where the A1 and A3 condition was applied, respectively. (c) and (d) are graphene grown on a 127 μm-thick electropolished copper foil for 5 min where the A1 and LPCVD process condition was applied, respectively. The scale bars are 5 μm.

Generally, hexagon-shape was commonly observed in the APCVD process [22,24–26], as in Fig. 5(c), while lobe-shaped dendritic morphology was noted in the LPCVD process [20,21] likewise Fig. 5(d). The hexagonal shape was interpreted as an equilibrium form for correlation with the hexagonal atomic structure of graphene. To account for this morphology, little effect from the Cu substrate on a graphene flake was considered [22] and low enough initial growth rate was suggested as a process requirement [26]. In contrast, the lobe-shape shown in the LPCVD process was attributed to the different crystallographic symmetry between a fourfold (100) Cu substrate and a sixfold graphene flake [21]. Although the shape of the graphene flakes appear to be influenced by many different factors, such as pressure [22], substrate [21], H_2/CH_4 ratio [23], the similar graphene flake shape between the A3 condition and LPCVD suggested that the growth kinetics of A3 (hydrogen excluded growth under AP) is different from typical APCVD (such as the result shown in Fig. 5(a) and (c)), but is similar to the LPCVD process, which is known to be dominated by surface reactions [14].

2.4.2. *The role of hydrogen in hydrogen-excluded APCVD process*

Recently, the role of hydrogen in the graphene growth on Cu foil was also discussed by Vlassiouk et al. [23]. It was found that no matter the growth ambient is AP or LP, the shape of nuclei could evolve from a random shape into a hexagonal shape with the increase of hydrogen concentration. Unfortunately, for the growth under AP, in order to obtain uniform single layer graphene, the discussion had focused on the regime with highly diluted methane (~30 ppm). In this regime, hydrogen serves both as an auxiliary catalyst and an etchant for graphene, leading to form the hexagonal shape by the balance between the two roles with sufficient hydrogen concentration. The investigation carried out in this work appeared to be outside the regime discussed in the earlier work [23]. Nevertheless, much light is shed upon the current result from the discussion there. It is known that without hydrogen gas in the reaction mixture, methane has to chemisorb on the copper surface to form active carbon species to produce graphene. Such dehydrogenation reactions are not thermodynamically favorable thus constitutes the rate limiting step [27]. As a result, the growth kinetics of A3 (hydrogen excluded growth) becomes surface reaction-limited. Furthermore, the insensitivity of surface topography was understood that since the surface reaction on a copper foil is relatively difficult, the catalytic effect by copper is more important, not involving any topological factor of surface. The hexagonal shape was favored in the kinetically mass transport-limiting regime where lower interaction between graphene and copper was expected [22,26] whereas the lobed shape that can be regarded as a kind of dendritic growth was mostly observed in the kinetically surface reaction-limiting regime where the graphene growth along a specific direction could be limited by an interaction with the copper [21].

2.5. *The characterization of electric properties along with graphene passivated etch test*

Finally, the electric property of the single layer graphene grown by A3 condition was investigated. Monolayer graphene sample grown by LPCVD (detailed description of the

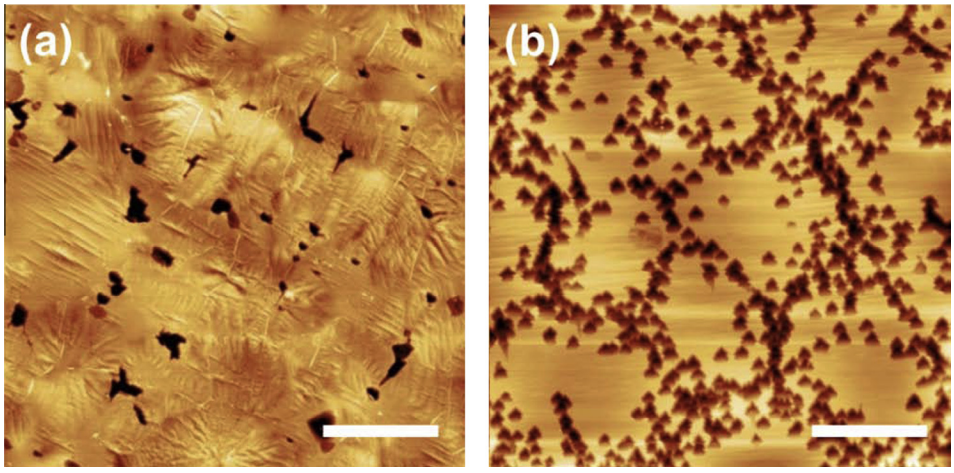

Fig. 6 – AFM image taken after a graphene passivated etch test on a copper foil. (a) The graphene grown by A3 condition. The AFM image before this etch test is given in Fig. S4(a) in Supporting Information. (b) The graphene grown by LPCVD process. Higher density of etch pits were observed than in (a). The scale bars are 5 μm.

process was given in Supporting Information) process was used for comparison. The graphene samples were transferred onto SiO_2/Si substrates for the characterization. For the graphene grown by the hydrogen-excluded APCVD process, the sheet resistance and mobility obtained from a four-point measurement were 289.8 ohm/□ and 1271.8 cm^2/(V s), respectively while for the graphene grown by the LPCVD process, values of 305.3 ohm/□ and 825.9 cm^2/(V s), were obtained. Further measurements were carried out and consistently to be relatively better performances were obtained for the APCVD samples. Furthermore, graphene passivated etch test was carried out to evaluate the openings in the graphene film [28]. The technique was simple that a copper etchant (Transence APS-100) droplet was brought onto an as-grown graphene sample using a plastic pipette. After 5 s, the drop of etchant was rinsed away with deionized water and the sample was quickly dried by blowing compressed nitrogen. Detailed usage of this technique was described elsewhere [28]. Fig. 6(a) and (b) show the results of this etching test conducted in the graphene grown by the hydrogen-excluded APCVD process and the LPCVD process, respectively. Remarkably, the etch pits were commonly observed although the density of pits in Fig. 6(a) was much lower than Fig. 6(b). This observation informed the graphene grown by CVD process is basically not possible to perfectly passivate copper surface [29,30]. Meanwhile, since no etch pit with a significant size was not found, both of the graphenes were regarded to have a full coverage over copper. The origin of these pits was attributed to incomplete coverage of graphene [20] or nanoparticle presumed to be an oxide [23]. Since the structural defects can be regarded as the most sensitive factor to process condition among these, the difference of density of etch pits shown in Fig. 6 could be correlated to the domain size to a certain extent. In fact, the distribution of etch pits in Fig. 6(b) appeared to give form borders between distinct regions, but any certain evidence that these regions denoted to the graphene domains was not found yet. Nevertheless, since it is still obvious that a graphene with larger domain size can lead to have less lattice defects, the average domain size of the graphene in Fig. 6(a) was considered to be larger than the one in Fig. 6(b). Furthermore, the earlier observation that better electric properties were noted in the sample prepared this APCVD process also supported this speculation because the domain boundary is considered as a blocking factor against electronic transport, lowering the electron mobility [25]. The formation of graphene with large domain size requires relatively less nucleation rate and higher growth rate because the domain boundary would be determined when graphene flakes coalescence each other. As mentioned earlier, the partially grown graphene prepared by the hydrogen-excluded APCVD process showed the less nucleus density and higher growth rate [31] than the one by the hydrogen-introduced APCVD process. This can be accounted for the hydrogen that could promote the nucleation of graphene as a supporting catalyst [23] and lower the growth rate by suppressing the dissociation of methane. Although the measurement of exact domain size will be followed to compare with the graphene grown by the LPCVD process that can have a domain size up to 0.5 mm [12], this remarkably simple hydrogen-excluded APCVD process provides a promising process condition that can lead to synthesize a pristine monolayer graphene with high quality and full coverage over copper foil with less complicated and expensive system than LPCVD.

3. Conclusion

In conclusion, the graphene morphology grown by APCVD process was investigated with respect to the hydrogen introduction in each synthesis step. Remarkably, a pristine monolayer graphene was resulted when the simplest condition where hydrogen was excluded in all the steps was applied. This morphology variation of graphene was understood by discerning the role of hydrogen in APCVD. The multilayer graphene formed along the rolling line direction of copper foil was attributed to the combination of surface roughening of copper by hydrogen-induced annealing

and mass transport-limiting kinetics in the hydrogen-induced CVD process. On the other hand, a pristine monolayer observed in the hydrogen-excluded process with less sensitivity on the methane concentration and structural irregularities, led to a postulation that the dominant kinetics is surface reaction limiting, which is similar to LPCVD. This was confirmed by comparing the domain shape of partially grown graphene. We concluded that the shape of nuclei was closely associated with the dominating kinetics determined by hydrogen in the APCVD, refining a previous report on the role of hydrogen. Finally, in the characterization of electric properties and graphene passivated etch test, better performances were presented in the graphene by hydrogen-excluded APCVD process than the one prepared by the LPCVD process. This hydrogen-excluded APCVD process is expected to provide a simpler way to synthesize high quality graphene in large area.

Conflict of interest

The authors declare no competing financial interests.

Acknowledgment

This work was partially supported by National Science Foundation under award number NSF DMR 0845358 and the Graphene Approaches to Terahertz Electronics (GATE) Multidisciplinary University Research Initiative (MURI) of Massachusetts Institute of Technology (MIT)-Harvard University-Boston University through the Office of Naval Research (ONR). Y.C.S planned and carried out all the experiments. Y.C.S. thanks Dr. Mario Hofmann and Dr. Daniel Nezich for their preceding experimental developments applied in this study. Y.C.S. and J. K acknowledge Dr. Mildred Dresselhaus for comments on this work.

Appendix A. Supplementary data

Supplementary data associated with this article can be found, in the online version, at http://dx.doi.org/10.1016/j.carbon.2013.03.037.

REFERENCE

[1] Novoselov KS, Geim AK, Morozov SV, Jiang D, Zhang Y, Dubonos SV, et al. Electric field effect in atomically thin carbon films. Science 2004;306(5696):666–9.
[2] Morozov SV, Novoselov KS, Katsnelson MI, Schedin F, Elias DC, Jaszczak JA, et al. Giant intrinsic carrier mobilities in graphene and its bilayer. Phys Rev Lett 2008;100(1):016602.
[3] Elias DC, Nair RR, Mohiuddin TMG, Morozov SV, Blake P, Halsall MP, et al. Control of graphene's properties by reversible hydrogenation: evidence for graphane. Science 2009;323(5914):610–3.
[4] Gomez-Navarro C, Burghard M, Kern K. Elastic properties of chemically derived single graphene sheets. Nano Lett 2008;8(7):2045–9.
[5] Balandin AA, Ghosh S, Bao W, Calizo I, Teweldebrhan D, Miao F, et al. Superior thermal conductivity of single-layer graphene. Nano Lett 2008;8(3):902–7.
[6] Wang Y, Tong SW, Xu XF, Oezyilmaz B, Loh KP. Interface engineering of layer-by-layer stacked graphene anodes for high-performance organic solar cells. Adv Mater 2011;23(13):1514–8.
[7] Lin YM, Dimitrakopoulos C, Jenkins KA, Farmer DB, Chiu HY, Grill A, et al. 100-GHz transistors from wafer-scale epitaxial graphene. Science 2010;327(5966):662.
[8] Lin YM, Valdes-Garcia A, Han SJ, Farmer DB, Meric I, Sun YN, et al. Wafer-Scale Graphene Integrated Circuit. Science 2011;332(6035):1294–7.
[9] Bae S, Kim H, Lee Y, Xu X, Park J-S, Zheng Y, et al. Roll-to-roll production of 30-inch graphene films for transparent electrodes. Nat Nanotechnol 2010;5(8):574–8.
[10] Zhu Y, Murali S, Stoller MD, Ganesh KJ, Cai W, Ferreira PJ, et al. Carbon-based supercapacitors produced by activation of graphene. Science 2011;332(6037):1537–41.
[11] Reina A, Jia XT, Ho J, Nezich D, Son HB, Bulovic V, et al. Large area, few-layer graphene films on arbitrary substrates by chemical vapor deposition. Nano Lett 2009;9(1):30–5.
[12] Li X, Cai W, An J, Kim S, Nah J, Yang D, et al. Large-area synthesis of high-quality and uniform graphene films on copper foils. Science 2009;324(5932):1312–4.
[13] Kim KS, Zhao Y, Jang H, Lee SY, Kim JM, Kim KS, et al. Large-scale pattern growth of graphene films for stretchable transparent electrodes. Nature 2009;457(7230):706–10.
[14] Bhaviripudi S, Jia XT, Dresselhaus MS, Kong J. Role of kinetic factors in chemical vapor deposition synthesis of uniform large area graphene using copper catalyst. Nano Lett 2010;10(10):4128–33.
[15] Luo Z, Lu Y, Singer DW, Berck ME, Somers LA, Goldsmith BR, et al. Effect of substrate roughness and feedstock concentration on growth of wafer-scale graphene at atmospheric pressure. Chem Mater 2011;23(6):1441–7.
[16] Nair RR, Blake P, Grigorenko AN, Novoselov KS, Booth TJ, Stauber T, et al. Fine structure constant defines visual transparency of graphene. Science 2008;320(5881):1308.
[17] Blake P, Brimicombe PD, Nair RR, Booth TJ, Jiang D, Schedin F, et al. Graphene-based liquid crystal device. Nano Lett 2008;8(6):1704–8.
[18] Li XS, Zhu YW, Cai WW, Borysiak M, Han BY, Chen D, et al. Transfer of large-area graphene films for high-performance transparent conductive electrodes. Nano Lett 2009;9(12):4359–63.
[19] Hutchings FR, Unterweiser PM. Failure Analysis the British Engine Technical Reports. American Society for Metals; 1981. pp. 249–61.
[20] Li X, Magnuson CW, Venugopal A, An J, Suk JW, Han B, et al. Graphene films with large domain size by a two-step chemical vapor deposition process. Nano Lett 2010;10(11):4328–34.
[21] Wofford JM, Nie S, McCarty KF, Bartelt NC, Dubon OD. Graphene islands on cu foils: the interplay between shape, orientation, and defects. Nano Lett 2010;10(12):4890–6.
[22] Robertson AW, Warner JH. Hexagonal single crystal domains of few-layer graphene on copper foils. Nano Lett 2011;11(3):1182–9.
[23] Vlassiouk I, Regmi M, Fulvio P, Dai S, Datskos P, Eres G, et al. Role of hydrogen in chemical vapor deposition growth of large single-crystal graphene. ACS Nano 2011;5(7):6069–76.
[24] Ajayan PM, Yakobson BI. Graphene pushing the boundaries. Nat Mater 2011;10(6):415–7.
[25] Yu Q, Jauregui LA, Wu W, Colby R, Tian J, Su Z, et al. Control and characterization of individual grains and grain boundaries in graphene grown by chemical vapour deposition. Nat Mater 2011;10(6):443–9.
[26] Wu B, Geng D, Guo Y, Huang L, Xue Y, Zheng J, et al. Equiangular hexagon-shape-controlled synthesis of graphene on copper surface. Adv Mater 2011;23(31):3522–5.

[27] Zhang W, Wu P, Li Z, Yang J. First-principles thermodynamics of graphene growth on Cu surfaces. J Phys Chem C 2011;115(36):17782–7.
[28] Hofmann M, Shin YC, Hsieh Y-P, Dresselhaus MS, Kong J. A facile tool for the characterization of two-dimensional materials grown by chemical vapor deposition. Nano Res 2012;5(7):504–11.
[29] Chen S, Brown L, Levendorf M, Cai W, Ju S-Y, Edgeworth J, et al. Oxidation resistance of graphene-coated Cu and Cu/Ni alloy. ACS Nano 2011;5(2):1321–7.
[30] Nemes-Incze P, Yoo KJ, Tapaszto L, Dobrik G, Labar J, Horvath ZE, et al. Revealing the grain structure of graphene grown by chemical vapor deposition. Appl Phys Lett 2011;99(2):023104-1–4.
[31] Gao L, Ren W, Zhao J, Ma L-P, Chen Z, Cheng H-M. Efficient growth of high-quality graphene films on Cu foils by ambient pressure chemical vapor deposition. Appl Phys Lett 2010;97(18):183109-1–3.